Jurnal ELTIKOM :
Jurnal Teknik Elektro, Teknologi Informasi dan Komputer

Vol. 8, No. 2, December 2024, page. 163-178
ISSN 2598-3245 (Print), ISSN 2598-3288 (Online)
DOI: http://doi.org/10.31961/eltikom.v8i2.1290
Available online at http://eltikom.poliban.ac.id

OPTIMAL POWER FLOW USING AN OPTIMALLY TUNED PATTERN SEARCH ALGORITHM

Firmansyah Nur Budiman[1*], Taufal Hidayat[2,3], Rudi Uswarman[3,4]
[1)] Department of Electrical Engineering, Universitas Islam Indonesia, Yogyakarta, Indonesia
[2)] Department of Electrical Engineering, Institut Teknologi Padang, Padang, Indonesia
[3)] Department of Electrical and Computer Engineering, King Abdulaziz University, Jeddah, Saudi Arabia
[4)] Department of Electrical Engineering, Institut Teknologi Sumatera, Lampung Selatan, Indonesia
e-mail: firmansyah.nur@uii.ac.id, taufalhidayat4690@gmail.com, uswarman@el.itera.ac.id

Received: 19 August 2024 – Revised: 11 November 2024 – Accepted: 11 November 2024

ABSTRACT

Optimal power flow (OPF) is a critical optimization application in power system planning and operation. Numerous studies employ metaheuristic techniques to address OPF problems of varying complexity. However, these techniques often suffer from slow convergence due to their dependence on the quality of initial solutions. To overcome this limitation, initial solutions must be optimally tuned to achieve good outcomes with faster convergence. This paper proposes an optimally tuned pattern search (OPS) algorithm to solve OPF problems in medium and large power systems. The tuning process, performed using the classical interior point method (IPM), provides optimal initial control variable values for the standard pattern search (PS) algorithm. The proposed technique is applied to three test systems: IEEE 30-bus, IEEE 57-bus, and IEEE 118-bus systems. The OPF problem is formulated to minimize four objectives: total active power loss, total generator fuel cost, total generator emission, and total deviation in load bus voltage magnitude. The performance of the OPS algorithm is evaluated based on objective function values and computation times and is compared with IPM and two popular metaheuristic techniques, particle swarm optimization (PSO) and genetic algorithm (GA). Results indicate that the OPS algorithm's performance varies across test systems but generally balances optimization performance with computational efficiency.

Keywords*: optimal power flow, optimally tuned pattern search, power system optimization.*

I. INTRODUCTION

OPTIMAL power flow (OPF) is one of the most complex problems in power systems. It is applied in routine operations, generation and transmission expansion planning, network resiliency, and market analysis [1], [2]. Compared to other analyses such as load flow analysis and economic dispatch problems, OPF is significantly more computationally demanding [3]. OPF is an optimization process aimed at minimizing one or several quantities within the system. It incorporates load flow equations to calculate fundamental quantities such as voltage and power, making the problem nonlinear and nonconvex due to the nature of these equations. During optimization, constraints related to power balance, voltage limits, and power generation limits must be satisfied.

The nonconvexity and nonlinearity of the OPF problem pose significant challenges for classical optimization techniques, such as the interior-point method (IPM) and Newton's method [4]. This has prompted the adoption of metaheuristic optimization techniques, which aim to achieve global optimality and improve local optima for OPF problems [5]. A wide range of metaheuristic algorithms has been applied to OPF problems, including tabu search (TS) [6], differential evolution (DE) [7], genetic algorithms (GA) and their modified versions [8], boosting cuckoo algorithms [9], particle swarm optimization (PSO) [10], gravitational search algorithms [11], [12], teaching-learning based optimization (TLBO) [13], chaotic bat algorithms [14], heap optimization [15], mayfly algorithms [16], artificial bee colony algorithms [17], and animal migration algorithms [18]. These techniques are employed to minimize one or more objective functions, such as total power loss, fuel cost, voltage deviation, or emissions.

TABLE 1
CONTROL AND DEPENDENT VARIABLES USED IN THE STUDY

Control Variables		Dependent Variables	
P_G	Active power generation at PV buses	P_{Gs}	Active power generation at the slack bus
V_G	Voltage magnitude at generator buses, including the slack bus	V_L	Voltage magnitude at load buses
T	Tap setting of transformers	Q_G	Reactive power generation at generator buses including the slack bus
Q_C	Shunt MVAR compensation		

Consequently, OPF can be formulated as either a single-objective or a multi-objective optimization problem.

Despite the advantages of the metaheuristic techniques mentioned earlier, they generally suffer from relatively high computation times due to the process of generating random populations. This is because metaheuristic techniques typically require initial values, and the quality of these initial solutions is not always adequate, meaning they are often far from optimal. One potential approach to enhance the efficiency and effectiveness of the population generation process is to use solutions provided by faster classical techniques as initial values. Such a hybrid technique has been explored in [19], [20].

This paper aims to apply a hybrid technique to address the OPF problem in medium and large power systems. The main contribution of this study is the introduction of a novel hybrid approach, referred to as the optimally tuned pattern search (OPS) algorithm. This hybrid technique combines the classical interior-point method (IPM) with the standard pattern search (PS) algorithm. In this study, the proposed technique is applied to four different cases, each targeting the minimization of a distinct objective: power loss, fuel cost, generation emissions, and load bus voltage deviation. The objectives of this study are as follows: to apply the OPS algorithm for OPF with four different objective functions and compare its performance, in terms of objective function minimization, with those achieved by IPM, PSO, and GA; and to evaluate the OPS algorithm for OPF with four different objective functions and compare its computational performance, in terms of computation time, with those of IPM, PSO, and GA. The proposed technique is particularly beneficial for addressing OPF in large power systems, where both speed and solution accuracy are critical.

The structure of the paper is as follows. Section IIA presents the OPF problem formulation used in this study. Section IIB provides a brief overview of the PS algorithm and describes how IPM enhances its performance. Section IIC discusses the application of the proposed technique to the selected test systems. Section III presents the results and discussion. Finally, Section IV concludes the study and suggests potential improvements for future research.

II. RESEARCH METHOD

A. Problem Formulation

A standard OPF problem can be formulated as a constrained nonlinear optimization problem, as expressed in (1) which is subject to (2) and (3) where x represents the vector of control variables, u represents the vector of dependent variables, $J(\mathrm{x}, \mathrm{u})$ is the objective function to optimize, $g(\mathrm{x}, \mathrm{u}) = 0$ is the set of equality constraints, and $h(\mathrm{x}, \mathrm{u}) \leq 0$ is the set of inequality constraints. The control and dependent variables for each test system used in this study are presented in Table 1.

Both control and dependent variables must remain within their respective maximum and minimum limits [21]. This requirement is mathematically defined by the constraints in (4)-(10) where P_G is the active power generation at generator bus, P_{Gs} is the active power generation at the slack bus, V_G is the voltage magnitude at the generator bus, Q_C is the MVAR supplied by the shunt device, T is the tap setting of the transformer, V_L is the voltage at load bus, N_G is the number of generator buses (including the swing bus), N_C is the number of shunt devices, N_T is the number of tap-changing transformers, and N_L is the number of load buses.

Equations (4)-(7) pertain to the control variables, while Equations (8)-(10) pertain to the dependent variables. Note that (4) assumes the slack bus is located at bus 1 for simplicity in notation. This assumption is solely for convenience and does not limit the applicability of the formulation to systems with a slack bus at any other location. The enforcement of the dependent variable limits in Equations (8)-(10) is implemented by incorporating a penalty function into the objective function. This penalty function is defined as shown in (11) where λ_P, λ_V, and λ_Q are the penalty factors. The value $u^{\lim}$, representing the violated limit of the dependent variable u, is defined in (12).

$$\text{Minimize } J(\mathbf{x},\mathbf{u}) \tag{1}$$

$$g(\mathbf{x},\mathbf{u}) = 0 \tag{2}$$

$$h(\mathbf{x},\mathbf{u}) \leq 0 \tag{3}$$

$$P_{Gi}^{\min} \leq P_{Gi} \leq P_{Gi}^{\max} \qquad i = 2,\dots,N_G \tag{4}$$

$$V_{Gi}^{\min} \leq V_{Gi} \leq V_{Gi}^{\max} \qquad i = 1,2,\dots,N_G \tag{5}$$

$$T_i^{\min} \leq T_i \leq T_i^{\max} \qquad i = 1,2,\dots,N_T \tag{6}$$

$$Q_{Ci}^{\min} \leq Q_{Ci} \leq Q_{Ci}^{\max} \qquad i = 1,2,\dots,N_C \tag{7}$$

$$P_{Gs}^{\min} \leq P_{Gs} \leq P_{Gs}^{max} \tag{8}$$

$$V_{Li}^{\min} \leq V_{Li} \leq V_{Li}^{\max} \qquad i = 1,2,\dots,N_L \tag{9}$$

$$Q_{Gi}^{\min} \leq Q_{Gi} \leq Q_{Gi}^{\max} \qquad i = 1,2,\dots,N_G \tag{10}$$

$$\text{Penalty} = \lambda_P\left(P_{Gs} - P_{Gs}^{\lim}\right)^2 + \lambda_V\sum_{i=1}^{N_L}\left(V_{Li} - V_{Li}^{\lim}\right)^2 + \lambda_Q\sum_{i=1}^{N_G}\left(Q_{Gi} - Q_{Gi}^{\lim}\right)^2 \tag{11}$$

$$u^{\lim} = \begin{cases} u^{\max} & u > u^{\max} \\ u^{\min} & u < u^{\min} \end{cases} \tag{12}$$

$$P_{loss} = \sum_{k=1}^{ntl} G_k\left[V_i^2 + V_j^2 - 2V_iV_j\cos\left(\theta_i - \theta_j\right)\right] \qquad \text{MW} \tag{13}$$

$$F = \sum_{k=1}^{N_G} a_i + b_iP_{Gi} + c_iP_{Gi}^2 \qquad \$/\text{h} \tag{14}$$

$$\text{Emission} = \sum_{k=1}^{N_G} \alpha_i + \beta_iP_{Gi} + \gamma_iP_{Gi}^2 + \omega_ie^{\mu_iP_{Gi}} \qquad \text{ton/h} \tag{15}$$

$$\text{Emission} = \sum_{k=1}^{N_G} \delta_iP_{Gi} \qquad \text{ton/h} \tag{16}$$

$$VD = \sum_{i=1}^{N_L} |V_L - 1| \tag{17}$$

This study minimizes four objective functions independently. The first objective function is the total active power loss, expressed by (13) where ntl is the number of transmission lines, i and j are the indices of the buses connected by line k, G_k is the conductance of line k, V_i is the voltage magnitude at bus i, V_j is the voltage magnitude at bus j, θ_i is the voltage angle at bus i, and θ_j is the voltage angle at bus j. The second objective function is the total generation fuel cost, given by (14) where a, b, and c are the cost coefficient of the generator. The third objective function is the total generation emission, for which two formulations are used. The first formulation is expressed in (15) where α, β, γ, ω, and μ are the emission coefficients of the generator. The second formulation, a simplified linear model [22], is expressed in (16). As detailed in Section II.C, (15) and (16) are applied to different test systems. The fourth objective function is the deviation of load bus voltage magnitude from the nominal value. Given that the nominal bus voltage is 1 pu, this deviation is formulated in (17).

The objective functions in (13)-(17) depend on bus power injection and bus voltage, which are obtained from the load flow study. Therefore, the load flow computation accompanies the construction of these objective functions, as illustrated in Figure 1. From an optimization perspective, both control and dependent variables contribute to the objective functions defined in (13)-(17). As shown in Figure 1, some variables have a direct impact on the objective function, while others influence the function indirectly through load flow computations. For instance, in the case of active power loss, the variables that

TABLE 2
FORMULATIONS OF OBJECTIVE FUNCTIONS USED IN THE STUDY

Case	Objective Function
Case 1	$J(x,u) = P_{\text{loss}} + \text{Penalty}$
Case 2	$J(x,u) = F + \text{Penalty}$
Case 3	$J(x,u) = \text{Emission} + \text{Penalty}$
Case 4	$J(x,u) = VD + \text{Penalty}$

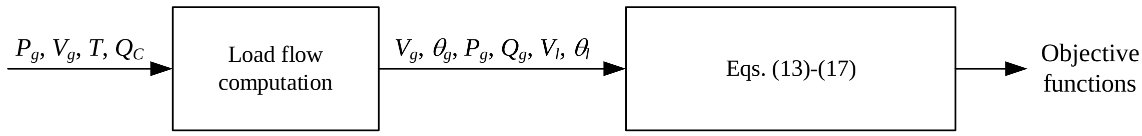

Figure 16. Construction of the objective functions used in the study

directly affect the loss are the voltages at the generator buses V_g and their associated angles θ_g, as well as the voltages at the load buses V_l and their associated angles θ_l. Consequently, other variables do not directly influence the power loss.

To simplify the problem formulation, the OPF problems with the four objective functions in (13)-(17) are categorized as Case 1, Case 2, Case 3, and Case 4. With the inclusion of the penalty function, the objective functions for these cases are summarized in Table 2.

To evaluate the effectiveness of the proposed technique, in addition to using the OPS algorithm, all OPF problems described above are also solved using three other algorithms: IPM, PS, and GA. The MATLAB implementation of these algorithms for the formulated problems is detailed in Section IIC. For each case and algorithm, the achieved objective function value and the computation time required to solve the problem are recorded. An algorithm is considered successful if it converges to optimal or near-optimal values and ensures that all dependent variables remain within the specified limits. This criterion is also examined during the study.

B. Pattern Search Algorithm

The Pattern Search (PS) algorithm is a metaheuristic optimization method classified as a direct search technique [23]. It is widely used to solve gradient-free optimization problems. As a direct search method, PS employs a straightforward search process involving the sequential evaluation of trial solutions. This sequence creates a mesh around the initial solution and iteratively approaches an optimal solution. Each trial solution is compared to the best solution obtained so far, guiding the selection of subsequent trial solutions. This process ensures convergence to near-optimal solutions.

The algorithm begins by generating a random point, which serves as the initial solution and is designated as the first base point. In subsequent iterations, another random trial point is selected for exploratory evaluation and compared to the preceding solution. If the fitness function value of the trial point is better, it replaces the previous base point. In such cases, an expansion coefficient is applied to generate new solutions, increasing the mesh size. Conversely, if the trial point does not yield a better fitness value, a contraction coefficient is applied, reducing the mesh size. The process terminates when the mesh size becomes smaller than a predefined threshold. For a more detailed explanation of the PS algorithm, readers are referred to [23].

As with other algorithms, the speed of convergence depends significantly on the initial solutions, which serve as the first base points [24], [25]. Solutions closer to the optimal values facilitate faster convergence. To achieve this condition, optimal initial values are provided to the algorithm by first solving the OPF problems using the Interior Point Method (IPM). The solutions from IPM are then used as the initial solutions for the PS algorithm, creating the optimally tuned Pattern Search (OPS) algorithm. The performance of OPS is compared to that of three other algorithms in this study.

C. Application and Implementation

The problem formulated in Section IIA is applied to three test systems: IEEE 30-bus, IEEE 57-bus, and IEEE 118-bus. Data for the IEEE 30-bus and IEEE 57-bus systems are sourced from [26], while data for the IEEE 118-bus system are obtained from [27]. These datasets include bus, branch, and generator data (such as cost coefficients and emission coefficients). The main characteristics of these systems are summarized in Tables 3, 4, and 5. As outlined in Section IIA, two formulations are used for the emission functions: Expressions (15) and (16). Expression (15), which is nonconvex and nonlinear, is

TABLE 3
MAIN CHARACTERISTICS OF THE IEEE 30-BUS SYSTEM

System Characteristics	Number	Details
Buses	30	[28]
Branches	41	[28]
Generators	6	Buses: 1, 2, 5, 8, 11, and 13
Shunts	9	Buses: 10, 12, 15, 17, 20, 21, 23, 24, and 29
Tap-changing transformers	4	Branches: 6-9, 6-10, 4-12, and 28-27
Control variables	24	-
Dependent variables	31	-

TABLE 4
MAIN CHARACTERISTICS OF THE IEEE 57-BUS SYSTEM

System Characteristics	Number	Details
Buses	57	[28]
Branches	80	[28]
Generators	7	Buses: 1, 2, 3, 6, 8, 9, and 12
Shunts	3	Buses: 18, 25, and 53
Tap-changing transformers	17	Branches: 4-18, 4-18, 21-20, 24-25, 24-25, 24-26, 7-29, 34-32, 11-41, 15-45, 14-46, 10-51, 13-49, 11-43, 40-56, 39-57, 9-55
Control variables	33	-
Dependent variables	58	-

TABLE 5
MAIN CHARACTERISTICS OF THE IEEE 118-BUS SYSTEM

System Characteristics	Number	Details
Buses	118	[29]
Branches	186	[29]
Generators	54	Buses: 1, 4, 6, 8, 10, 12, 15, 18, 19, 24, 25, 26, 27, 31, 32, 34, 36, 40, 42, 46, 49, 54, 55, 56, 59, 61, 62, 65, 66, 69, 70, 72, 73, 74, 76, 77, 80, 85, 87, 89, 90, 91, 92, 99, 100, 103, 104, 105, 107, 110, 111, 112, 113, 116
Shunts	14	Buses: 5, 34, 37, 44, 45, 46, 48, 74, 79, 82, 83, 105, 107, 110
Tap-changing transformers	9	Branches: 8-5, 26-25, 30-17, 38-37, 63-59, 64-61, 65-66, 68-69, 81-80
Control variables	130	-
Dependent variables	119	-

TABLE 6
CONTROL PARAMETERS FOR THE ALGORITHMS USED IN THE STUDY

Algorithm / Solver	Control Parameter	Value			Description
		30-bus	57-bus	118-bus	
IPM (fmincon)	Maximum number of function evaluations	3000	3000	100000	Iterations end when any of these values are reached
	Maximum number of iterations	1000	1000	1000	
	Termination tolerance on the first-order optimality	10-6	10-6	10-6	
	Termination tolerance on x, that is a lower bound on the size of a step	10-10	10-10	10-10	
	Tolerance on the constraint violation	10-6	10-6	10-6	
PSO	Number of particles in the swarm	100	100	100	-
	Maximum number of iterations	4800	6600	26000	Iterations end when this value is reached
	Termination tolerance on the function value	10-6	10-6	10-6	Iterations end when the relative changes in the best objective function value over n_i iterations are less than termination tolerance on the function value
	Maximum number of stall iterations n_i	20	20	20	
GA	Tolerance on the constraint violation	10-3	10-3	10-3	Iterations end when any of these values are reached
	Maximum number of generations	2400	3300	13000	
	Termination tolerance on the function value	10-6	10-6	10-6	The algorithm stops if the average relative changes in the best fitness function value over n_g generations are less than or equal to termination tolerance on the function value
	Maximum number of stall generations n_g	50	50	50	
OPS	Tolerance on the constraint violation	10-6	10-6	10-6	Iterations stop when any of these values are reached
	Maximum number of iterations	2400	3300	13000	
	Tolerance on mesh size	10-6	10-6	10-6	
	Maximum number of objective function evaluations	48000	66000	260000	
	Termination tolerance on the function value	10-6	10-6	10-6	Iterations stop if the change in function value is less than this value and the mesh size is less than tolerance on the variable
	Tolerance on the variable	10-6	10-6	10-6	Iterations stop if both the change in position and the mesh size are less than tolerance on the variable

applied to the IEEE 30-bus and IEEE 57-bus systems. In contrast, Expression (16), which is linear, is applied to the IEEE 118-bus system.

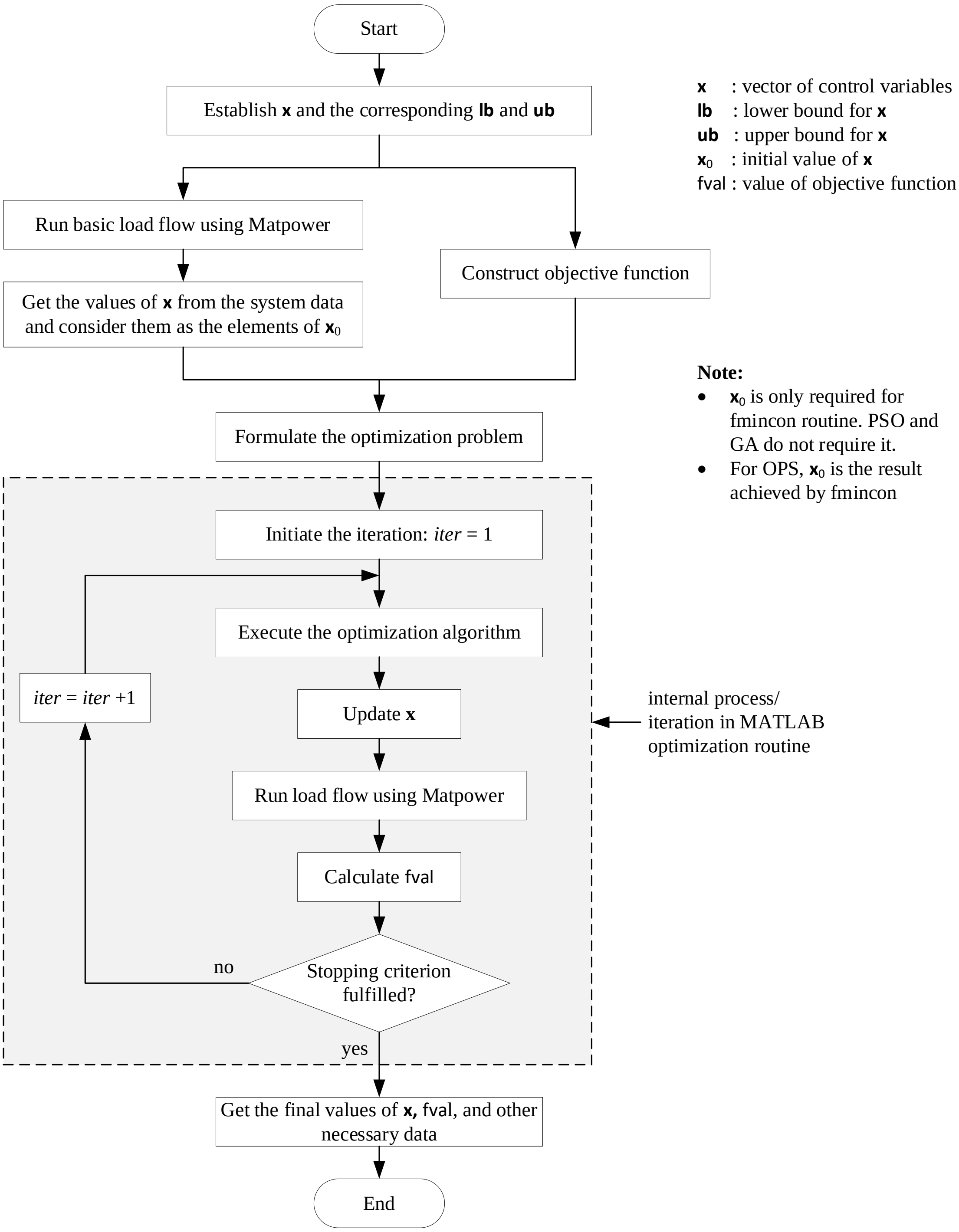

Figure 17. Framework of MATLAB implementation for each case and algorithm used in the study

The algorithms used in this study—IPM, PSO, GA, and the proposed OPS—are implemented in MATLAB, utilizing the Optimization and Global Optimization Toolboxes. Specifically, IPM, PSO, and GA are solved using the fmincon, particleswarm, and ga solvers, respectively.

In addition to the optimization routines, Matpower [30] is employed to perform the load flow computations required for constructing the objective functions. The initial values needed by fmincon are obtained from a basic state simulation, which involves using the primary data provided by the test systems without imposing dependent variable limits. Meanwhile, the OPS algorithm is solved using the patternsearch solver, with its initial values supplied by fmincon.

The framework of MATLAB implementation for each optimization routine (solver) and case used in this study is illustrated in the flowchart in Figure 2. The control parameters for the algorithms employed in this study are summarized in Table 6.

TABLE 7
RESULTS OF THE LOAD FLOW COMPUTATION ON THE IEEE 30-BUS SYSTEM AT BASIC STATE

Variable		Limit		Value	Variable		Limit		Value
		Low	High				Low	High	
Control variables					Dependent variables				
Generator bus voltage (pu)	V1	0.95	1.1	1.05	Voltage at load buses (pu)	V3	0.95	1.1	1.012
	V2	0.95	1.1	1.04		V4	0.95	1.1	1.003
	V5	0.95	1.1	1.01		V6	0.95	1.1	1.003
	V8	0.95	1.1	1.01		V7	0.95	1.1	0.998
	V11	0.95	1.1	1.05		V9	0.95	1.1	1.022
	V13	0.95	1.1	1.05		V10	0.95	1.1	1.005
Shunt MVAR	QC10	0	5	0		V12	0.95	1.1	1.033
	QC12	0	5	0		V14	0.95	1.1	1.016
	QC15	0	5	0		V15	0.95	1.1	1.009
	QC17	0	5	0		V16	0.95	1.1	1.014
	QC20	0	5	0		V17	0.95	1.1	1.003
	QC21	0	5	0		V18	0.95	1.1	0.995
	QC23	0	5	0		V19	0.95	1.1	0.990
	QC24	0	5	0		V20	0.95	1.1	0.993
	QC29	0	5	0		V21	0.95	1.1	0.993
Transformer tap	T6-9	0.9	1.1	0.978		V22	0.95	1.1	0.993
	T6-10	0.9	1.1	0.969		V23	0.95	1.1	0.994
	T4-12	0.9	1.1	0.932		V24	0.95	1.1	0.983
	T28-27	0.9	1.1	0.968		V25	0.95	1.1	0.990
Power generation at PV buses (MW)	PG2	20	80	40		V26	0.95	1.1	0.972
	PG5	15	50	0		V27	0.95	1.1	1.003
	PG8	10	35	0		V28	0.95	1.1	1.000
	PG11	10	30	0		V29	0.95	1.1	0.983
	PG13	12	40	0		V30	0.95	1.1	0.971
					P_{slack} (MW)	PG1	50	200	261.693
					Reactive power generation at generator buses (MVAR)	QG1	0	10	-29.972
Quantities to optimize						QG2	-40	50	66.908
P_{loss} (MW)				18.293		QG5	-40	40	42.090
VD (pu)				0.266		QG8	-10	40	57.051
F ($/h)				878.198		QG11	-6	24	14.369
Emission (ton/h)				0.908		QG13	-6	24	12.468

D. *Assumptions and Limitations*

This section outlines the assumptions and limitations associated with the proposed algorithm. In this study, the focus is on the algorithm itself; therefore, the proposed algorithm is tested only on conventional power systems, i.e., systems without any integration of renewable energy sources. Nonetheless, the proposed algorithm can be extended to systems that include renewable energy technologies, such as solar photovoltaics and wind turbines.

Two scenarios arise when considering the inclusion of renewable energy. In the first scenario, uncertainties associated with renewable energy technologies are ignored, assuming their output powers are perfectly predictable. Under this assumption, buses with renewable energy technologies are treated as voltage-controlled buses. Consequently, the computational complexity remains largely unchanged, as the only new components introduced are additional voltage-controlled buses.

In the second scenario, the uncertainties in renewable energy outputs are accounted for, requiring the use of stochastic optimization techniques. In such cases, the problem becomes more complex, as the uncertain outputs from renewable sources must be modeled as random variables. While the proposed algorithm can still be applied, its effectiveness will depend on how these random variables are managed—a consideration beyond the scope of this study and the proposed algorithm.

III. RESULTS AND DISCUSSION

This section presents and discusses the results for each test system. For each system, the load flow computation results at the basic state are provided first, followed by the optimization results. The performance of the proposed OPS algorithm is analyzed in two aspects: objective function value minimization and computation time. Additionally, performance charts are included to visualize and compare the OPS algorithm's performance with other algorithms used in this study. All computations were performed on an 11th Gen 1.40 GHz Core i7 personal computer with 32 GB of RAM.

TABLE 8
OPTIMAL VALUES OF CONTROL VARIABLES FOR IEEE 30-BUS SYSTEM AT CASE 1 AND CASE 2

Variable	Case 1				Case 2			
	IPM	PSO	GA	OPS	IPM	PSO	GA	OPS
V1	1.073	1.100	1.079	1.073	1.100	1.100	1.100	1.100
V2	1.063	1.093	1.071	1.067	1.079	1.081	1.085	1.080
V5	1.043	1.075	1.055	1.047	1.053	1.054	1.050	1.055
V8	1.052	1.082	1.062	1.052	1.062	1.062	1.039	1.063
V11	1.053	1.100	1.100	1.100	1.093	1.100	1.061	1.100
V13	1.053	1.100	1.100	1.093	1.087	1.100	1.047	1.100
QC10	2.616	5.000	4.999	5.000	3.599	4.994	1.338	5.000
QC12	2.554	4.998	5.000	5.000	3.476	4.992	0.069	5.000
QC15	2.659	4.288	4.998	5.000	3.527	4.976	1.897	5.000
QC17	2.679	5.000	5.000	5.000	3.914	4.999	4.123	5.000
QC20	2.691	3.524	3.944	4.269	3.625	4.343	4.396	4.299
QC21	2.774	5.000	4.999	5.000	4.230	4.999	4.970	5.000
QC23	2.708	2.272	2.584	2.770	3.284	2.814	2.558	2.698
QC24	2.866	5.000	5.000	5.000	4.268	5.000	4.970	5.000
QC29	2.562	2.019	2.069	2.199	2.534	2.381	2.395	2.314
T6-9	0.998	1.050	1.013	1.003	1.002	1.022	1.023	1.029
T6-10	0.987	0.901	0.902	0.900	0.939	0.900	0.940	0.900
T4-12	1.006	0.984	0.968	0.947	0.972	0.965	0.969	0.973
T28-27	0.990	0.969	0.949	0.942	0.965	0.953	0.977	0.956
PG2	73.232	80.000	80.000	80.000	48.606	48.656	51.486	48.602
PG5	48.252	50.000	50.000	50.000	21.326	21.342	21.583	21.304
PG8	32.749	35.000	35.000	35.000	20.980	20.997	22.442	21.012
PG11	27.853	30.000	30.000	30.000	12.010	11.899	12.154	11.850
PG13	36.529	40.000	39.999	40.000	12.299	12.002	12.076	12.000
P_{loss} (MW)	3.535	2.843	2.928	2.953	8.667	8.617	8.754	8.629
F ($/h)	931.200	967.048	967.251	967.313	799.297	799.035	800.651	799.046
Emission (ton/h)	0.221	0.221	0.221	0.221	0.368	0.368	0.356	0.369
VD (pu)	0.701	2.043	1.959	1.906	1.641	1.978	0.926	1.929

TABLE 9
OPTIMAL VALUES OF CONTROL VARIABLES FOR IEEE 30-BUS SYSTEM AT CASE 3 AND CASE 4

Variable	Case 3				Case 4			
	IPM	PSO	GA	OPS	IPM	PSO	GA	OPS
V1	1.048	1.099	1.065	1.047	1.045	1.015	1.043	1.045
V2	1.030	1.091	1.052	1.039	1.026	1.008	1.021	1.026
V5	1.013	1.072	1.023	1.020	1.012	1.009	1.000	1.012
V8	1.021	1.079	1.030	1.028	1.001	1.006	0.998	1.001
V11	1.030	1.098	1.069	1.096	1.044	1.042	1.079	1.044
V13	1.029	1.100	1.068	1.099	1.033	1.001	1.024	1.033
QC10	2.705	4.898	0.258	5.000	2.502	5.000	0.209	0.193
QC12	3.082	0.004	4.920	5.000	2.979	0.233	0.332	0.000
QC15	2.923	4.887	4.535	5.000	2.772	4.998	5.000	0.016
QC17	2.750	4.329	4.937	5.000	2.513	0.162	0.009	0.000
QC20	2.768	3.748	3.671	4.349	2.468	5.000	5.000	5.000
QC21	2.685	4.740	4.947	5.000	2.439	4.998	3.041	5.000
QC23	2.775	2.003	2.980	2.690	2.536	4.762	4.915	5.000
QC24	2.638	4.996	4.948	5.000	2.501	5.000	4.999	5.000
QC29	2.406	2.192	2.707	2.260	2.504	0.609	0.000	1.458
T6-9	0.997	1.048	1.004	0.956	0.985	1.059	0.953	0.985
T6-10	1.000	0.901	0.951	0.901	0.979	0.900	1.045	0.979
T4-12	1.003	0.965	1.057	0.933	0.999	0.965	1.009	0.999
T28-27	0.999	0.966	0.979	0.920	0.958	0.949	0.944	0.958
PG2	47.765	70.835	71.067	70.903	49.965	79.990	32.313	25.568
PG5	33.473	50.000	49.985	50.000	29.613	49.999	15.011	29.613
PG8	28.575	35.000	34.945	35.000	23.548	34.980	10.006	20.613
PG11	21.315	30.000	29.941	30.000	18.511	30.000	28.580	30.000
PG13	35.720	32.822	32.811	32.822	28.415	39.995	12.067	17.631
P_{loss} (MW)	5.942	3.103	3.496	3.329	7.188	3.547	10.879	8.052
F ($/h)	842.311	932.837	933.936	933.521	821.371	968.661	820.379	826.233
Emission (ton/h)	0.262	0.217	0.218	0.217	0.287	0.222	0.428	0.340
VD (pu)	0.322	2.013	0.710	1.787	0.183	0.096	0.156	0.146

A. IEEE 30-Bus System

Table 7 shows the results of the load flow computation for the IEEE 30-bus system at the basic state. The table includes the values of control variables, dependent variables, and the four quantities to be optimized. It is important to note that the load flow computation at this state does not enforce the limits on dependent variables. Consequently, many dependent variable values exceed their permissible limits.

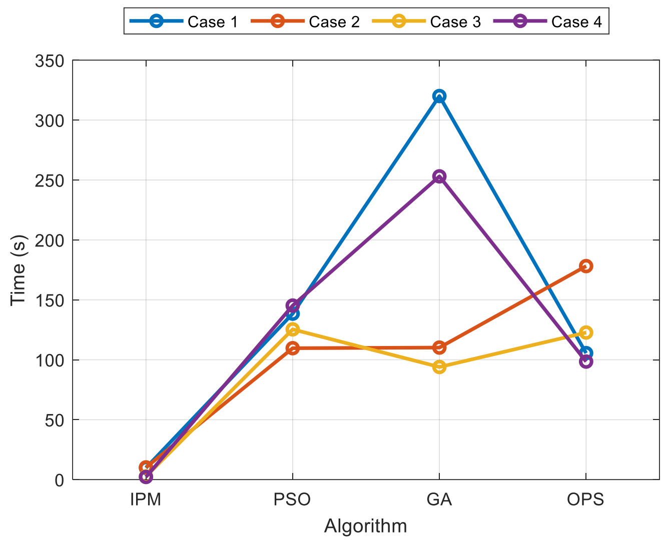

Figure 18. Computation Time for Simulation on IEEE 30-Bus System

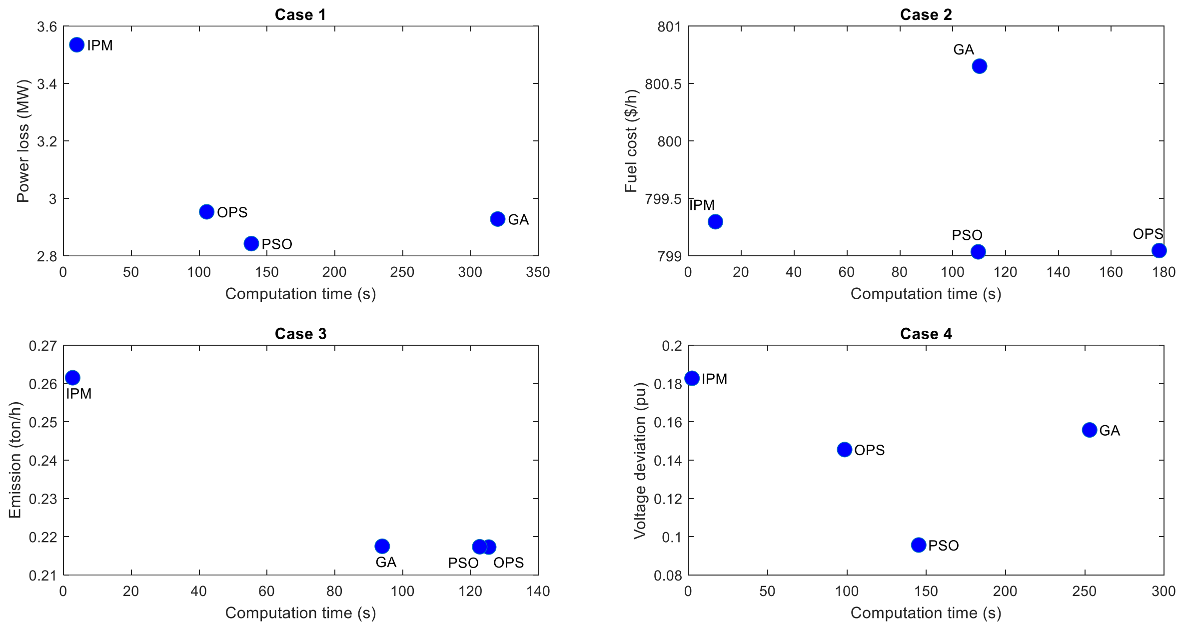

Figure 19. Performance Charts of OPF on IEEE 30-Bus System

Therefore, the optimization process not only aims to minimize the objective function values but also ensures that all dependent variable values are within the allowable range as defined by the constraints.

The optimized values of control variables and objective functions are presented in Tables 8 and 9. For the IEEE 30-bus system, no violations of dependent variable limits are observed, indicating that all algorithms are successful in meeting the constraints. The comparison of objective function value minimization among the algorithms is conducted for each case.

Across all cases, the proposed OPS and other algorithms successfully reduce the objective function values compared to those at the basic state. However, a general trend is observed: PSO, GA, and the proposed OPS consistently outperform IPM by significant margins, except in Case 2, where GA exhibits the poorest performance. PSO emerges as the top performer in all cases, followed by the proposed OPS, except in Case 1, where it performs slightly worse than GA.

Figure 3 illustrates the computation times required by all algorithms. As shown, IPM is the fastest algorithm in all cases, with the proposed OPS being the second-fastest in most cases (except in Case 2). This indicates that for the IEEE 30-bus system, the proposed OPS offers a suitable trade-off between accuracy and computation time. Conversely, GA is the least recommended algorithm for this system (except in Case 3), given its ordinary performance in reducing objective function values and its poor computation time in most cases.

TABLE 10
RESULTS OF THE LOAD FLOW COMPUTATION ON THE IEEE 57-BUS SYSTEM AT BASIC STATE

Variable		Limit Low	Limit High	Value	Variable		Limit Low	Limit High	Value
Control variables					Dependent variables				
Generator bus voltage (pu)	V1	0.95	1.1	1.04	Voltage at load buses (pu)	V23	0.95	1.1	1.001
	V2	0.95	1.1	1.01		V24	0.95	1.1	0.984
	V3	0.95	1.1	0.985		V25	0.95	1.1	0.938
	V6	0.95	1.1	0.98		V26	0.95	1.1	0.945
	V8	0.95	1.1	1.005		V27	0.95	1.1	0.973
	V9	0.95	1.1	0.98		V28	0.95	1.1	0.990
	V12	0.95	1.1	1.015		V29	0.95	1.1	1.004
Shunt MVAR	QC18	0	5	0		V30	0.95	1.1	0.920
	QC25	0	5	0		V31	0.95	1.1	0.900
	QC53	0	5	0		V32	0.95	1.1	0.926
Transformer tap	T4-18	0.9	1.1	0.97		V33	0.95	1.1	0.924
	T4-18	0.9	1.1	0.978		V34	0.95	1.1	0.949
	T21-20	0.9	1.1	1.043		V35	0.95	1.1	0.958
	T24-25	0.9	1.1	1		V36	0.95	1.1	0.968
	T24-25	0.9	1.1	1		V37	0.95	1.1	0.978
	T24-26	0.9	1.1	1.043		V38	0.95	1.1	1.007
	T7-29	0.9	1.1	0.967		V39	0.95	1.1	0.976
	T34-32	0.9	1.1	0.975		V40	0.95	1.1	0.965
	T11-41	0.9	1.1	0.955		V41	0.95	1.1	0.994
	T15-45	0.9	1.1	0.955		V42	0.95	1.1	0.963
	T14-46	0.9	1.1	0.9		V43	0.95	1.1	1.008
	T10-51	0.9	1.1	0.93		V44	0.95	1.1	1.012
	T13-49	0.9	1.1	0.895		V45	0.95	1.1	1.033
	T11-43	0.9	1.1	0.958		V46	0.95	1.1	1.057
	T40-56	0.9	1.1	0.958		V47	0.95	1.1	1.029
	T39-57	0.9	1.1	0.98		V48	0.95	1.1	1.023
	T9-55	0.9	1.1	0.94		V49	0.95	1.1	1.033
Power generation at PV buses (MW)	PG2	0	100	0		V50	0.95	1.1	1.021
	PG3	0	140	40		V51	0.95	1.1	1.051
	PG6	0	100	0		V52	0.95	1.1	0.968
	PG8	0	550	450		V53	0.95	1.1	0.955
	PG9	0	100	0		V54	0.95	1.1	0.987
	PG12	0	410	310		V55	0.95	1.1	1.028
Dependent variables						V56	0.95	1.1	0.964
Voltage at load buses (pu)	V4	0.95	1.1	0.978		V57	0.95	1.1	0.960
	V5	0.95	1.1	0.976	P_{slack} (MW)	PG1	0	575.9	479.262
	V7	0.95	1.1	0.982	Reactive power generation at generator buses (MVAR)	QG1	-140	200	129.833
	V10	0.95	1.1	0.986		QG2	-17	50	-0.751
	V11	0.95	1.1	0.973		QG3	-10	60	7.369
	V13	0.95	1.1	0.978		QG6	-8	25	6.010
	V14	0.95	1.1	0.969		QG8	-140	200	65.386
	V15	0.95	1.1	0.987		QG9	-3	9	6.862
	V16	0.95	1.1	1.013		QG12	-150	155	130.745
	V17	0.95	1.1	1.017					
	V18	0.95	1.1	0.975	Quantities to optimize				
	V19	0.95	1.1	0.951	P_{loss} (MW)				28.462
	V20	0.95	1.1	0.950	VD (pu)				1.554
	V21	0.95	1.1	1.000	F ($/h)				16895.095
	V22	0.95	1.1	1.003	Emission (ton/h)				2.416

The performance charts of the algorithms used in this study for the IEEE 30-bus system are presented in Figure 4. The chart for Case 1 highlights the advantage of the proposed OPS algorithm, demonstrating its ability to balance objective function value minimization and computation time. As a result, OPS positions itself between IPM and PSO in terms of overall performance. The chart also confirms the relative disadvantage of GA in this case. A similar pattern is observed in Case 4, where the proposed OPS effectively bridges the speed advantage of IPM with the accuracy advantage of PSO.

Different patterns emerge in Cases 2 and 3. In these cases, the proposed OPS exhibits the longest computation times. This drawback is not offset by superior results in terms of objective function values. OPS performs worse than PSO in both computation time and objective function value minimization. In Case 3, PSO also fails to outperform GA. Consequently, for minimizing fuel cost on the IEEE 30-bus system (Case 2), PSO is recommended as the best solver. For minimizing emissions (Case 3), GA is suggested as the most effective algorithm.

TABLE 11
OPTIMAL VALUES OF CONTROL VARIABLES FOR IEEE 57-BUS SYSTEM AT CASE 1 AND CASE 2

Variable	Case 1				Case 2			
	IPM	PSO	GA	OPS	IPM	PSO	GA	OPS
V1	1.055	1.010	1.039	1.047	1.053	1.100	1.013	1.079
V2	1.026	1.004	1.031	1.037	1.028	1.098	0.995	1.064
V3	1.013	1.010	1.032	1.030	1.015	1.090	0.992	1.019
V6	1.001	1.010	1.027	1.017	1.001	1.083	1.027	1.000
V8	1.003	1.014	1.022	1.004	1.005	1.096	1.057	0.999
V9	0.981	0.991	1.004	0.989	0.985	1.074	1.001	0.985
V12	1.013	0.997	1.016	1.009	1.018	1.090	0.993	1.010
QC18	4.999	5.000	5.000	5.000	0.014	5.000	4.997	5.000
QC25	4.994	5.000	5.000	5.000	4.468	5.000	4.998	5.000
QC53	2.148	5.000	5.000	5.000	4.182	4.999	4.999	5.000
T4-18	1.004	0.902	0.905	0.902	1.012	1.010	0.906	0.901
T4-18	1.023	0.902	0.933	0.929	0.970	0.946	0.903	0.907
T21-20	1.019	0.995	1.007	0.968	0.979	1.002	1.001	0.996
T24-25	0.956	0.949	0.946	0.901	0.973	0.919	0.918	0.910
T24-25	0.957	0.912	0.939	0.900	0.925	0.942	0.915	0.909
T24-26	1.039	0.992	1.031	1.016	1.062	0.970	1.028	0.968
T7-29	0.952	0.902	0.938	0.952	0.930	0.973	1.069	0.914
T34-32	0.968	0.919	0.929	0.900	0.928	0.920	0.906	0.912
T11-41	0.935	0.900	0.901	0.900	0.940	0.901	0.913	0.900
T15-45	0.956	0.900	0.914	0.944	0.971	0.973	0.900	0.908
T14-46	0.958	0.900	0.908	0.954	0.965	0.966	0.909	0.907
T10-51	0.900	0.906	0.910	0.933	0.900	0.990	0.954	0.920
T13-49	0.949	0.900	0.902	0.902	0.961	0.943	0.909	0.912
T11-43	0.937	0.900	0.900	0.900	0.951	0.965	0.913	0.900
T40-56	1.022	1.017	1.015	0.990	1.048	0.985	1.022	1.014
T39-57	0.994	0.985	0.985	0.959	0.966	0.943	0.982	0.979
T9-55	0.909	0.900	0.932	0.936	0.901	0.971	0.917	0.900
PG2	18.393	0.037	0.001	0.000	8.346	100.000	99.994	100.000
PG3	0.004	139.998	140.000	140.000	0.000	87.267	77.122	75.549
PG6	1.817	99.989	100.000	100.000	0.000	100.000	99.999	100.000
PG8	436.161	308.240	302.597	295.743	412.491	55.353	101.441	52.494
PG9	9.846	100.000	100.000	100.000	0.006	100.000	100.000	100.000
PG12	253.527	410.000	410.000	410.000	326.141	275.752	249.041	292.599
P_{loss} (MW)	35.427	10.516	10.321	11.095	30.848	43.436	52.410	45.722
F ($/h)	16083.19	11059.17	10857.48	10621.70	15150.99	5582.20	5802.47	5611.93
Emission (ton/h)	2.821	1.172	1.170	1.172	2.659	2.256	2.223	2.280
VD (pu)	1.128	2.207	2.348	1.446	1.089	3.375	1.415	2.087

B. IEEE 57-bus System

The load flow results for the IEEE 57-bus system at the basic state are presented in Table 10. Similar to the IEEE 30-bus system, several violations of dependent variable limits are observed, particularly in the voltage at load buses. The optimized values for the IEEE 57-bus system across all cases are shown in Tables 11 and 12. All algorithms successfully bring the dependent variables within permissible limits.

To evaluate the performance of the proposed OPS algorithm in terms of objective function value minimization, each case is analyzed. OPS ranks third among the four algorithms, but the differences in objective function values between OPS, PSO (the best), and GA (the second-best) are not significant. In Case 2, OPS improves to the second-best position, although it remains significantly different from the best-performing algorithm. Case 3 mirrors Case 1, where OPS ranks third with small differences between the best and second-best algorithms. Meanwhile, in Case 4, OPS surpasses IPM and GA, ranking second only to PSO.

The computation time performance for all algorithms is depicted in Figure 5. Apart from Case 2, the proposed OPS is the fastest among the three metaheuristic algorithms used in this study, although it remains slower than IPM. This slower speed is compensated by significantly better performance in objective function value minimization.

Figure 6 shows the performance charts for the algorithms on the IEEE 57-bus system. Compared to the charts for the IEEE 30-bus system, these charts exhibit a more uniform pattern across all cases, except for Case 2. The "balancing" advantage of OPS is evident in Cases 1, 3, and 4. In Case 2, while OPS is both slower and less accurate than PSO, the gaps in these parameters are not substantial.

C. IEEE 118-bus System

The results of the load flow computation for the IEEE 118-bus system at the basic state are presented in Table 13. A unique observation from the basic state simulation is the minimal number of violations

TABLE 12
OPTIMAL VALUES OF CONTROL VARIABLES FOR IEEE 57-BUS SYSTEM AT CASE 3 AND CASE 4

Variable	Case 1				Case 2			
	IPM	PSO	GA	OPS	IPM	PSO	GA	OPS
V1	1.040	1.031	1.026	1.033	1.039	1.035	1.012	1.039
V2	1.025	1.030	1.025	1.026	1.011	1.026	0.996	1.010
V3	1.003	1.025	1.023	1.003	1.004	1.021	1.003	1.004
V6	0.996	1.010	1.020	1.000	1.003	1.000	1.027	1.005
V8	1.012	1.011	1.028	1.005	1.013	1.025	1.062	1.017
V9	0.990	0.992	1.005	0.990	0.995	1.005	1.024	0.996
V12	1.027	1.002	1.011	1.011	1.037	1.018	1.041	1.036
QC18	2.876	4.976	4.996	5.000	4.625	4.873	0.083	5.000
QC25	4.606	5.000	4.998	5.000	4.394	5.000	5.000	4.791
QC53	4.991	5.000	5.000	5.000	2.884	5.000	5.000	5.000
T4-18	0.971	0.911	0.906	0.900	0.976	0.927	0.935	0.948
T4-18	0.980	0.911	0.931	0.900	0.978	1.066	0.980	0.947
T21-20	1.042	1.011	1.002	0.981	1.047	0.968	0.991	1.016
T24-25	0.964	0.932	0.910	0.901	0.967	0.900	0.928	0.975
T24-25	0.964	0.952	0.933	0.902	0.967	1.054	0.932	0.967
T24-26	1.044	1.006	1.024	1.028	1.047	1.036	1.008	1.039
T7-29	0.961	0.900	0.956	0.961	0.953	0.955	1.005	0.952
T34-32	0.964	0.931	0.920	0.902	0.975	0.916	0.946	0.918
T11-41	0.942	0.900	0.910	0.903	0.941	0.900	0.905	0.900
T15-45	0.952	0.903	0.913	0.921	0.946	0.900	0.910	0.929
T14-46	0.969	0.900	0.916	0.922	0.964	0.993	0.973	0.964
T10-51	0.900	0.900	0.934	0.947	0.936	1.000	1.021	0.965
T13-49	0.957	0.900	0.904	0.910	0.962	0.900	0.937	0.962
T11-43	0.943	0.900	0.909	0.900	0.947	0.965	0.918	0.932
T40-56	1.035	1.019	1.012	0.998	1.075	0.990	1.077	1.020
T39-57	0.947	0.987	0.981	0.962	0.945	0.906	0.986	0.937
T9-55	0.910	0.900	0.970	0.957	0.932	0.972	0.985	0.963
PG2	0.000	100.000	100.000	100.000	2.023	16.799	12.554	0.000
PG3	0.076	140.000	140.000	140.000	28.803	121.186	0.030	0.000
PG6	26.255	100.000	100.000	100.000	1.777	9.796	0.036	8.877
PG8	465.914	274.211	274.682	274.362	464.806	307.832	346.245	402.033
PG9	0.000	100.000	100.000	100.000	0.740	100.000	48.139	2.424
PG12	299.460	356.623	356.566	357.128	310.972	161.582	317.166	305.207
P_{loss} (MW)	28.168	13.505	13.759	14.412	27.620	40.144	35.009	33.130
F (\$/h)	17674.48	9588.22	9603.74	9599.04	17664.92	10510.20	12169.33	14624.66
Emission (ton/h)	2.506	0.955	0.956	0.957	2.416	2.406	2.605	2.789
VD (pu)	1.119	2.435	1.687	1.364	1.015	0.662	0.797	0.750

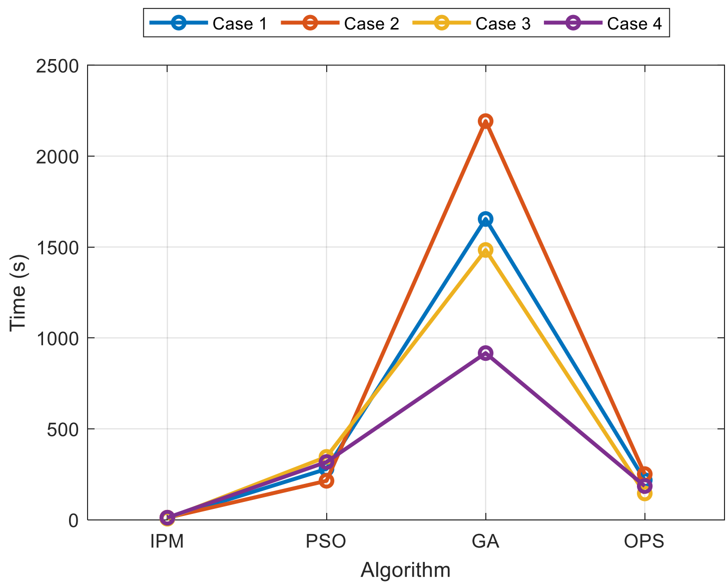

Figure 20. Computation Time for Simulation on IEEE 57-Bus System

of dependent variable limits. Out of 119 dependent variables, only six violate their limits, all of which pertain to reactive power generation at generator buses.

Table 14 shows the objective function values achieved by all algorithms for the IEEE 118-bus system across all cases. Notably, GA fails to ensure that all dependent variables remain within permissible limits during the simulation for this system. In fact, it introduces more violations than observed in the basic

TABLE 13
OBJECTIVE FUNCTION VALUES FOR IEEE 118-BUS SYSTEM AT BASIC STATE

Quantity	P_{loss} (MW)	F (\$/h)	Emission (ton/h)	VD (pu)
Value	133.357	131240.378	0.200	1.489

TABLE 14
OBJECTIVE FUNCTION VALUES FOR IEEE 118-BUS SYSTEM AT OPTIMIZED STATES

Quantities	Algorithm	Case 1	Case 2	Case 3	Case 4
P_{loss} (MW)	IPM	98.430	81.722	100.078	98.578
	PSO	12.783	93.200	242.812	127.334
	GA	156.896	156.883	146.554	193.288
	OPS	34.850	81.092	130.060	148.611
F (\$/h)	IPM	133528.157	132677.064	133519.129	133544.534
	PSO	166739.089	142321.631	201262.088	157638.202
	GA	156413.329	156767.475	160545.984	167682.212
	OPS	157086.138	132651.660	172317.454	147401.284
Emission (ton/h)	IPM	0.178	0.186	0.176	0.176
	PSO	0.180	0.179	0.043	0.204
	GA	0.134	0.175	0.186	0.180
	OPS	0.173	0.186	0.043	0.208
VD (pu)	IPM	3.248	3.714	2.675	3.138
	PSO	1.393	2.094	1.752	0.570
	GA	1.354	1.950	2.291	2.526
	OPS	3.353	3.847	2.959	2.631

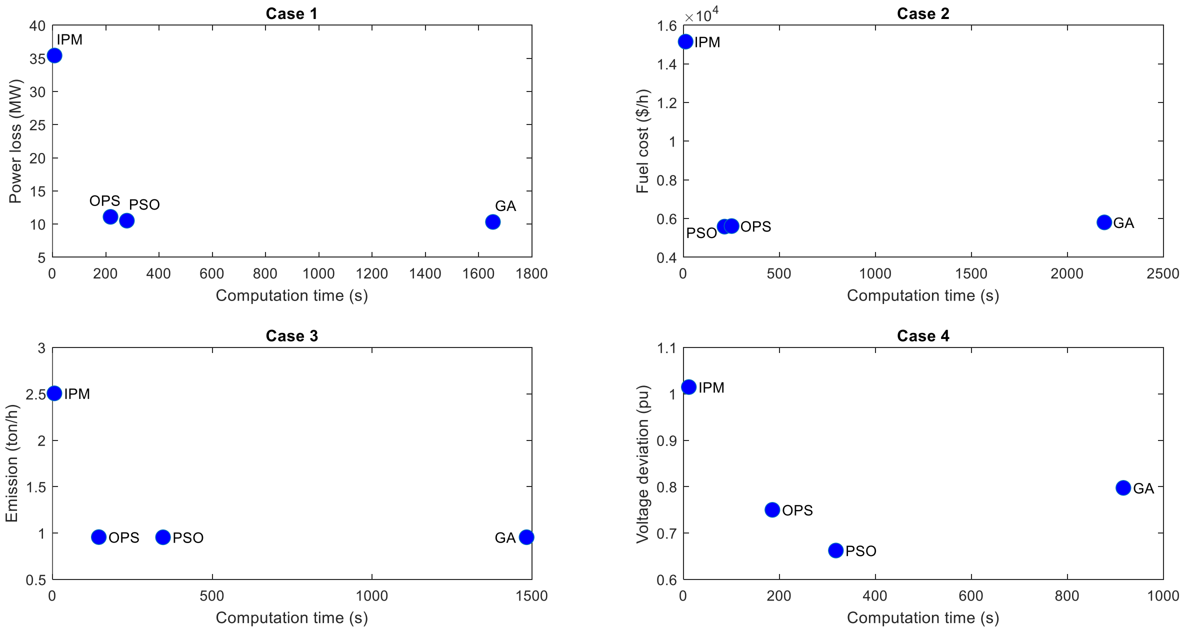

Figure 21. Performance Charts of OPF on IEEE 57-Bus System

state condition. This failure provides sufficient grounds to exclude GA from further consideration for the IEEE 118-bus system. Nevertheless, the results for GA are still presented to report its achieved objective function values and computation times.

In Case 1, the proposed OPS algorithm performs well, achieving the second-lowest power loss, with PSO outperforming it. In Case 2, the proposed OPS algorithm delivers the best performance, achieving the smallest fuel cost. It surpasses IPM and PSO, which rank second and third, respectively. A similar outcome is observed in Case 3, where OPS produces the best emission results, performing on par with PSO. However, in Case 4, OPS ranks third, trailing PSO and GA. As previously mentioned, GA's inability to resolve dependent variable limit violations diminishes its reliability, leaving OPS as the second-best option after PSO.

IPM remains the fastest algorithm, consistent with its performance in the IEEE 30-bus and IEEE 57-bus systems. Additionally, the proposed OPS algorithm outperforms the other two metaheuristic algorithms (PSO and GA) in Cases 1, 2, and 4. In Case 3, OPS ranks as the second-best algorithm, following PSO. The curves in Figure 7 further confirm GA's disadvantages when applied to the IEEE 118-bus system.

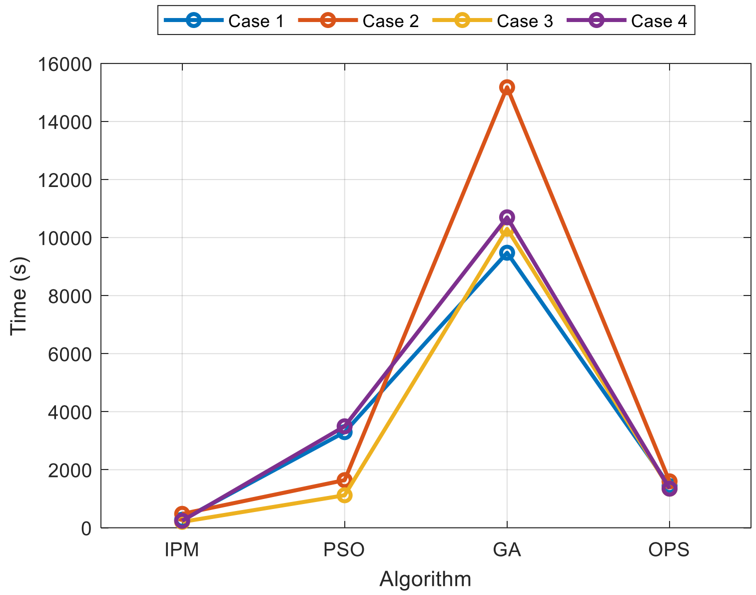

Figure 22. Computation Time for Simulation on IEEE 118-Bus System

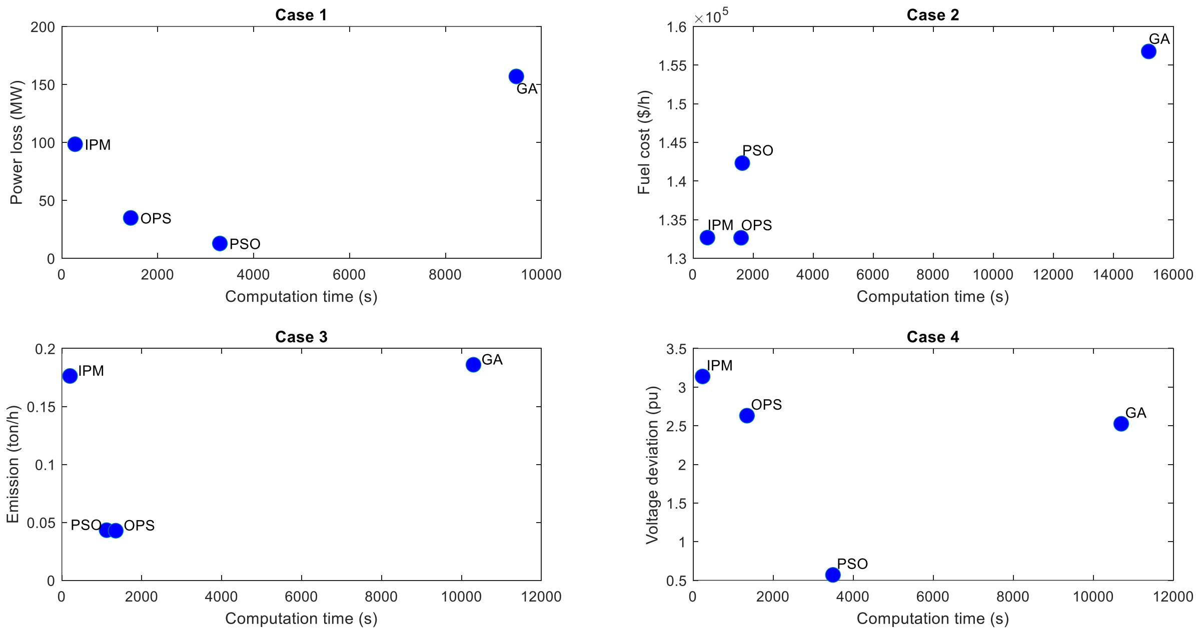

Figure 23. Performance Charts of OPF on IEEE 118-Bus System

The algorithm performance charts are illustrated in Figure 8. In Cases 1 and 4, the charts validate the proposed OPS algorithm's role as a balancer between speed and accuracy, consistently positioning it between IPM and PSO. In Case 2, OPS also ranks between IPM and PSO; however, IPM emerges as the best algorithm in this case. Interestingly, no algorithms successfully minimize the fuel cost in Case 2, as the "optimized" objective function values exceed the basic state values. Consequently, the three algorithms—IPM, PSO, and OPS—only accomplish one of the two objectives: forcing the dependent variables within permissible limits.

In Case 3, the proposed OPS algorithm lags behind PSO in both objective function value and computation time, ranking as the third-best algorithm. GA consistently performs the worst across all cases due to its slow computation and inability to meet the required performance criteria effectively.

IV. CONCLUSION

This study examined the solution of Optimal Power Flow (OPF) problems using the proposed OPS algorithm alongside three other algorithms on three different test systems. Each algorithm was applied to optimize four distinct objective functions for each system. The analysis revealed key insights into the performance of the OPS algorithm across various scenarios. The proposed OPS algorithm demonstrated a balance between accuracy and speed when minimizing power loss and bus voltage deviation. It was slower but more accurate than the Interior Point Method (IPM) and faster but slightly less accurate than Particle Swarm Optimization (PSO). This highlights its potential to effectively manage trade-offs between computation speed and optimization accuracy.

In cases where fuel cost was the objective function, the OPS algorithm's performance varied across the test systems. For the IEEE 30-bus system, OPS was the slowest algorithm and did not achieve a superior fuel cost value. For the IEEE 57-bus system, while slower than IPM, OPS obtained a better fuel cost value but was slightly less effective than PSO in terms of both computation time and cost optimization. For the IEEE 118-bus system, none of the algorithms minimized the fuel cost successfully, but all maintained dependent variables within permissible limits. In this scenario, OPS ranked between IPM and PSO in terms of both computation time and fuel cost value. When emission minimization was the objective, the OPS algorithm's performance again showed variability. For the IEEE 30-bus system, OPS was the slowest algorithm and did not achieve a superior emission value. In the IEEE 57-bus system, OPS effectively balanced the speed advantage of IPM and the accuracy of PSO. However, in the IEEE 118-bus system, OPS lagged behind PSO in both objective function value and computation time.

The study also evaluated the computation time of the OPS algorithm across different systems. For the IEEE 30-bus system, OPS was faster than the Genetic Algorithm (GA) in two cases but slower in the other two. For the IEEE 57-bus and IEEE 118-bus systems, OPS outperformed GA consistently. This suggests that OPS is better suited for medium and large systems due to its reliance on directional search strategies requiring fewer steps compared to GA's large search space and multiple generations. The use of IPM to generate the initial population for OPS did not significantly increase its computation time. When compared to IPM, the OPS algorithm was slower, which aligns with expectations, as IPM is among the fastest optimization algorithms for OPF problems. However, IPM's objective function minimization performance was generally weaker, making it more suitable for generating the initial population for OPS. In comparison with PSO, the performance varied depending on the test system and case. In some scenarios, OPS was faster than PSO, while in others, PSO outperformed OPS. This indicates that the OPS algorithm is comparable to PSO in terms of performance across the analyzed test systems, offering a promising alternative for solving OPF problems in various contexts.

This study does not address the integration of renewable energy technologies into the grid or the associated challenges, such as uncertainties and power quality. For future research, renewable energy technologies such as wind turbines and solar photovoltaics could be incorporated into the grid. Such studies could also model the uncertainties arising from the output power of these renewable sources, necessitating stochastic optimization approaches. Furthermore, renewable energy technologies, often installed alongside power electronics components, may impact power quality. Therefore, power quality issues could form another important area of investigation in future studies.

REFERENCES

[1] T. Wolgast and A. Nieße, "Learning the optimal power flow: Environment design matters," *Energy and AI*, vol. 17, p. 100410, Sep. 2024, doi: 10.1016/J.EGYAI.2024.100410.

[2] M. Ahmadipour, Z. Ali, V. K. Ramachandaramurthy, and H. M. Ridha, "A memory-guided Jaya algorithm to solve multi-objective optimal power flow integrating renewable energy sources," *Appl Soft Comput*, vol. 164, p. 111924, Oct. 2024, doi: 10.1016/J.ASOC.2024.111924.

[3] R. Mieth and H. V. Poor, "Prescribed robustness in optimal power flow," *Electric Power Systems Research*, vol. 235, p. 110704, Oct. 2024, doi: 10.1016/J.EPSR.2024.110704.

[4] A. Deihim, D. Apostolopoulou, and E. Alonso, "Initial estimate of AC optimal power flow with graph neural networks," *Electric Power Systems Research*, vol. 234, p. 110782, Sep. 2024, doi: 10.1016/J.EPSR.2024.110782.

[5] J. K. Skolfield and A. R. Escobedo, "Operations research in optimal power flow: A guide to recent and emerging methodologies and applications," *Eur J Oper Res*, vol. 300, no. 2, pp. 387–404, Jul. 2022, doi: 10.1016/J.EJOR.2021.10.003.

[6] K. Lenin, B. Ravindhranath Reddy, and M. Suryakalavathi, "Hybrid Tabu search-simulated annealing method to solve optimal reactive power problem," *International Journal of Electrical Power & Energy Systems*, vol. 82, pp. 87–91, Nov. 2016, doi: 10.1016/J.IJEPES.2016.03.007.

[7] K. M. Sallam, M. A. Hossain, S. Elsayed, R. K. Chakrabortty, M. J. Ryan, and M. A. Abido, "Optimal power flow considering intermittent solar and wind generation using multi-operator differential evolution algorithm," *Electric Power Systems Research*, vol. 232, p. 110377, Jul. 2024, doi: 10.1016/J.EPSR.2024.110377.

[8] A. Ebrahimi, R. Haghighi, H. Yektamoghadam, M. Dehghani, and A. Nikoofard, "Optimal Power Flow by Genetic Algorithm," in *Frontiers in Genetics Algorithm Theory and Applications*, M. Khosravy, N. Gupta, and O. Witkowski, Eds., Springer, Singapore, 2024, pp. 121–136. doi: 10.1007/978-981-99-8107-6_7.

[9] A. S. Alghamdi and M. A. Zohdy, "Boosting cuckoo optimization algorithm via Gaussian mixture model for optimal power flow problem in a hybrid power system with solar and wind renewable energies," *Heliyon*, vol. 10, no. 11, p. e31755, Jun. 2024, doi: 10.1016/J.HELIYON.2024.E31755.

[10] W. Bai, F. Meng, M. Sun, H. Qin, R. Allmendinger, and K. Y. Lee, "Differential evolutionary particle swarm optimization with orthogonal learning for wind integrated optimal power flow," *Appl Soft Comput*, vol. 160, p. 111662, Jul. 2024, doi: 10.1016/J.ASOC.2024.111662.

[11] C. Shilaja and T. Arunprasath, "Optimal power flow using Moth Swarm Algorithm with Gravitational Search Algorithm considering wind power," *Future Generation Computer Systems*, vol. 98, pp. 708–715, Sep. 2019, doi: 10.1016/J.FUTURE.2018.12.046.

[12] A. R. Bhowmik and A. K. Chakraborty, "Solution of optimal power flow using nondominated sorting multi objective gravitational search algorithm," *International Journal of Electrical Power & Energy Systems*, vol. 62, pp. 323–334, Nov. 2014, doi: 10.1016/J.IJEPES.2014.04.053.

[13] H. R. E. H. Bouchekara, M. A. Abido, and M. Boucherma, "Optimal power flow using Teaching-Learning-Based Optimization technique," *Electric Power Systems Research*, vol. 114, pp. 49–59, Sep. 2014, doi: 10.1016/J.EPSR.2014.03.032.

[14] S. Mugemanyi, Z. Qu, F. X. Rugema, Y. Dong, C. Bananeza, and L. Wang, "Optimal Reactive Power Dispatch Using Chaotic Bat Algorithm," *IEEE Access*, vol. 8, pp. 65830–65867, 2020, doi: 10.1109/ACCESS.2020.2982988.

[15] A. M. Shaheen, R. A. El-Sehiemy, H. M. Hasanien, and A. R. Ginidi, "An improved heap optimization algorithm for efficient energy management based optimal power flow model," *Energy*, vol. 250, p. 123795, Jul. 2022, doi: 10.1016/J.ENERGY.2022.123795.

[16] V. B. K, R. S, E. Verdú, K. K, and R. S P, "An optimal power flow solution to deregulated electricity power market using meta-heuristic algorithms considering load congestion environment," *Electric Power Systems Research*, vol. 214, p. 108867, Jan. 2023, doi: 10.1016/J.EPSR.2022.108867.

[17] X. He, W. Wang, J. Jiang, and L. Xu, "An Improved Artificial Bee Colony Algorithm and Its Application to Multi-Objective Optimal Power Flow," *Energies (Basel)*, vol. 8, no. 4, pp. 2412–2437, Mar. 2015, doi: 10.3390/EN8042412.

[18] S. P. Dash, K. R. Subhashini, and P. Chinta, "Development of a Boundary Assigned Animal Migration Optimization algorithm and its application to optimal power flow study," *Expert Syst Appl*, vol. 200, p. 116776, Aug. 2022, doi: 10.1016/J.ESWA.2022.116776.

[19] W. Bai, K. Y. Lee, and I. Eke, "Optimal Power Flow Considering Global Voltage Stability Based on a Hybrid Modern Heuristic Technique," *IFAC-PapersOnLine*, vol. 55, no. 9, pp. 413–418, Jan. 2022, doi: 10.1016/J.IFACOL.2022.07.072.

[20] V. Roberge and M. Tarbouchi, "Hybrid Method Based on Metaheuristics and Interior Point for Optimal Power Flow," in *5th International Conference on Intelligent Computing in Data Sciences*, Fez, Morocco: Institute of Electrical and Electronics Engineers Inc., Oct. 2021. doi: 10.1109/ICDS53782.2021.9626722.

[21] R. Rusilawati, "Pembentukan Kurva Kapabilitas Generator Menggunakan Pendekatan Sistem Modified Single Machine to Infinite Bus (M-SMIB) untuk Batasan Optimisasi Sistem Pembangkitan," *Jurnal ELTIKOM : Jurnal Teknik Elektro, Teknologi Informasi dan Komputer*, vol. 4, no. 2, pp. 132–139, Oct. 2020, doi: 10.31961/ELTIKOM.V4I2.225.

[22] R. Azizipanah-Abarghooee, V. Terzija, F. Golestaneh, and A. Roosta, "Multiobjective Dynamic Optimal Power Flow Considering Fuzzy-Based Smart Utilization of Mobile Electric Vehicles," *IEEE Trans Industr Inform*, vol. 12, no. 2, pp. 503–514, Apr. 2016, doi: 10.1109/TII.2016.2518484.

[23] O. Bozorg-Haddad, M. Solgi, and H. A. Loaiciga, *Meta-heuristic and evolutionary algorithms for engineering optimization*. Hoboken, NJ: John Wiley and Sons, Inc., 2017.

[24] X. Guo, J. Hu, H. Yu, M. Wang, and B. Yang, "A new population initialization of metaheuristic algorithms based on hybrid fuzzy rough set for high-dimensional gene data feature selection," *Comput Biol Med*, vol. 166, p. 107538, Nov. 2023, doi: 10.1016/J.COMPBIOMED.2023.107538.

[25] Q. Li, S. Y. Liu, and X. S. Yang, "Influence of initialization on the performance of metaheuristic optimizers," *Appl Soft Comput*, vol. 91, p. 106193, Jun. 2020, doi: 10.1016/J.ASOC.2020.106193.

[26] A. E. Chaib, H. R. E. H. Bouchekara, R. Mehasni, and M. A. Abido, "Optimal power flow with emission and non-smooth cost functions using backtracking search optimization algorithm," *International Journal of Electrical Power & Energy Systems*, vol. 81, pp. 64–77, Oct. 2016, doi: 10.1016/J.IJEPES.2016.02.004.

[27] M. R. Narimani, R. Azizipanah-Abarghooee, B. Zoghdar-Moghadam-Shahrekohne, and K. Gholami, "A novel approach to multi-objective optimal power flow by a new hybrid optimization algorithm considering generator constraints and multi-fuel type," *Energy*, vol. 49, no. 1, pp. 119–136, Jan. 2013, doi: 10.1016/J.ENERGY.2012.09.031.

[28] A. E. Chaib, H. R. E. H. Bouchekara, R. Mehasni, and M. A. Abido, "Optimal power flow with emission and non-smooth cost functions using backtracking search optimization algorithm," *International Journal of Electrical Power & Energy Systems*, vol. 81, pp. 64–77, Oct. 2016, doi: 10.1016/J.IJEPES.2016.02.004.

[29] L. Slimani and T. Bouktir, "Economic power dispatch of power systems with pollution control using artificial bee colony optimization," *Turkish Journal of Electrical Engineering and Computer Sciences*, vol. 21, no. 6, pp. 1515–1527, Jan. 2013, doi: 10.3906/elk-1106-10.

[30] R. D. Zimmerman, C. E. Murillo-Sánchez, and R. J. Thomas, "MATPOWER: Steady-state operations, planning, and analysis tools for power systems research and education," *IEEE Transactions on Power Systems*, vol. 26, no. 1, pp. 12–19, Feb. 2011, doi: 10.1109/TPWRS.2010.2051168.